Quantum Simulation of the Schwinger Model

Massless & Massive – Bosonized

Aman Goyal and Nikshay Chugh

November 25, 2025

Table of Contents

Massless Schwinger Model

Theory I: Hilbert Space & Physical States

The physical Hilbert space is defined by the constraint of Gauss' Law on the fermion Fock space. [1]

1. Gauss' Law Operator on Fock Space :

$$G(x) = Qe\delta(x) \tag{1}$$

2. Physical State Condition:

$$G(x)|state\rangle = 0 \implies \text{Charge } Q|state\rangle = 0 \tag{2}$$

3. Vacuum Structure (Chirality Sectors): The vacuum is a product of positive and negative chirality sectors, labeled by integer levels N_+ and N_-:

$$|vac; N_+ N_-\rangle = |vac; N_+\rangle_+ |vac; N_-\rangle_- \tag{3}$$

4. Charges:

$$Q = N_+ - N_- \quad , \quad Q_5 = N_+ + N_- - \frac{ecL}{\pi} \tag{4}$$

Theory II: Large Gauge Transformations & θ-Vacuum

The vacuum structure is non-trivial due to the topology of the gauge group $\pi_1(U(1)) = \mathbb{Z}$.

1. Large Gauge Transformation (Winding Number): A transformation with winding number 1 shifts the vacuum index:

$$|ground; N\rangle \longrightarrow |ground; N+1\rangle \tag{5}$$

2. The θ-Vacuum (Sec 5): To diagonalize the Hamiltonian and Large Gauge Transformations simultaneously, we construct the θ-vacuum:

$$|\theta\rangle \equiv \sum_N e^{-iN\theta}|ground; N\rangle \tag{6}$$

3. Modified Chiral Charge: Symmetry is generated by $\tilde{Q}_5$, which is conserved but not gauge invariant:

$$\tilde{Q}_5 \equiv Q_5 + \frac{ecL}{\pi} = N_+ + N_- \tag{7}$$

Theory III: Charge Screening Mechanism

Introducing external static charges reveals the screening properties of the massless Schwinger model (Sec 6).

1. External Current Source:

$$j_{ex,0}(x) = q(\delta(x - x_0) - \delta(x - y_0)) \tag{8}$$

2. Modified Gauss' Law:

$$\partial_x \left(-i \frac{\delta}{\delta A(x)} \right) = e(j_0(x) + j_{ex,0}(x)) \tag{9}$$

3. Interaction Energy (Yukawa Potential): The energy of the ground state with external charges shows exponential screening (mass generation), rather than a linear Coulomb potential:

$$E_0(x_0 - y_0) = \frac{(eq)^2}{2M} \left(1 - e^{-M|x_0 - y_0|} \right) \tag{10}$$

Results I: Field Evolution Heatmaps

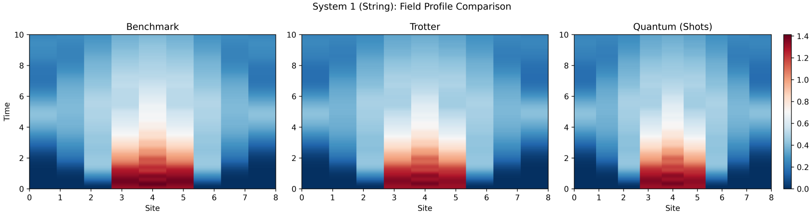

Comparison of Field $\langle \phi \rangle$ evolution: Benchmark vs. Quantum

System 1: String $(+q - q)$ from site 3-5.

Results II: Field Evolution Heatmaps

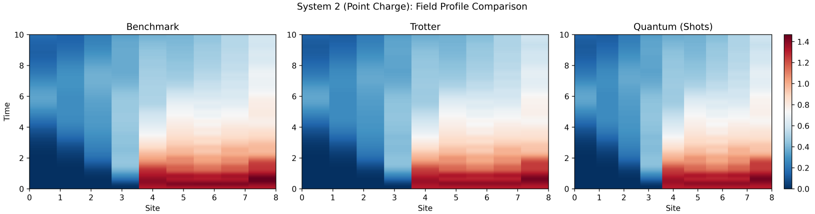

Comparison of Field $\langle \phi \rangle$ evolution: Benchmark vs. Quantum

System 2: Point charge $(+q)$ at site 4.

Results III: Induced Current Dynamics

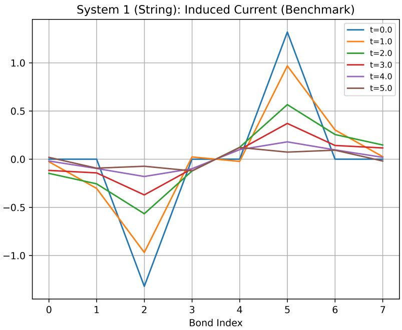

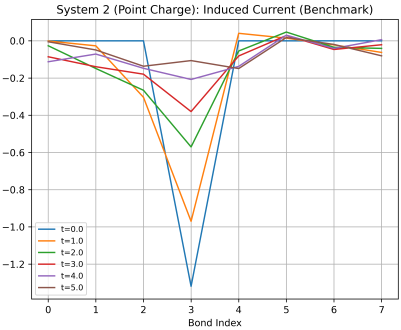

Current flow across lattice bonds over time

Results IV: Mid-Bond Charge Accumulation

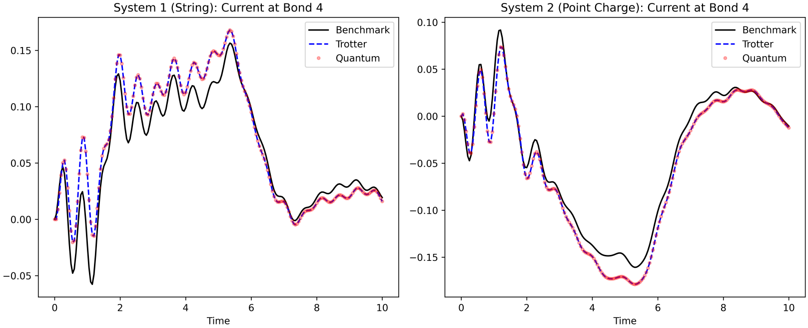

Evolution of Charge Density at the exact center of the lattice (Bond 4).

Discussion: Dynamics & Finite Size Effects

1. **Physical Interpretation ($J \propto -\Delta\phi$)**
   - This metric tracks **local charge accumulation**, not spatial flow.
2. **System 1 (String) - Breathing Mode**
   - The flux tube (string) is unstable and undergoes expansion/contraction.
   - **Boundary Reflection:** Sharp "beating" patterns at $t \approx 4$ indicate the wavefront reflecting off the lattice boundaries (Sites 0 & 8).
3. **System 2 (Point Charge) - Screening**
   - **Vacuum Polarization:** The deep negative dip represents the formation of a screening cloud to neutralize the domain wall.
   - **Massive Ringing:** The subsequent oscillations follow Bessel function behavior ($J_0(M\tau)$), characteristic of a massive boson settling into a screened state.

Results V: Massless Dynamics ($m = 0.0$)

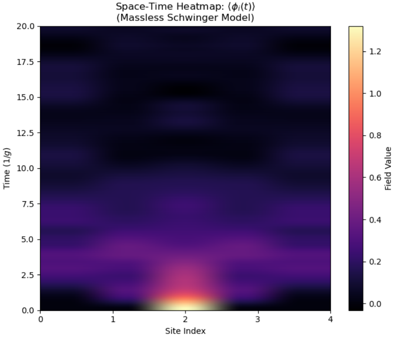

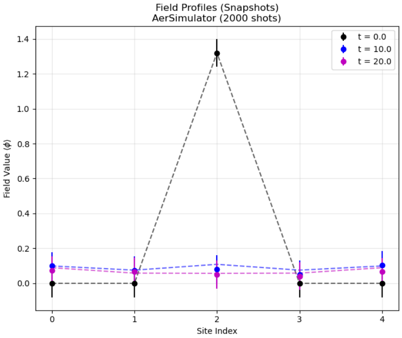

Observation: String Breaking / Dispersion

- Initial excitation at the center spreads rapidly outward ("light cone").
- The field value $\langle \phi \rangle$ decays towards constant as energy dissipates into massless pairs.

Massive Schwinger Model

Results VI: Massive Dynamics ($m = 0.5$)

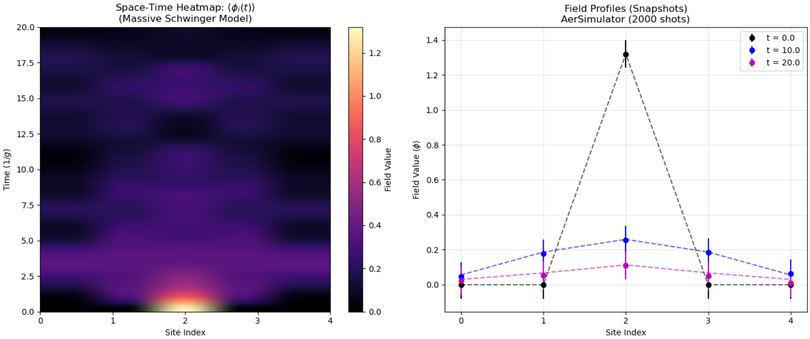

Observation: Confinement / Trapping

- The excitation keeps coming back to center. [2, 3]
- The non-linear mass term $-mg\cos(2\sqrt{\pi}\phi)$ acts as a confining potential, preventing the "string" from fully breaking.

Discussion: Effect of Fermion Mass

The heatmaps visualize the difference between screening and confinement.

1. **Massless Limit ($m = 0$)**
   - Theory: Free Massive Scalar Boson (mass $\mu = e/\sqrt{\pi}$).
   - Physics: The vacuum efficiently screens the external charge. The energy density disperses freely.
2. **Massive Limit ($m = 0.5$)**
   - Theory: Sine-Gordon Model (Interacting).
   - Physics: Creating screening pairs now costs mass energy ($2m$).
   - Result: The flux tube is "trapped" or stable on short timescales, exhibiting coherent oscillations rather than decay.

Results VII: Massless Dynamics ($m = 0.0$)

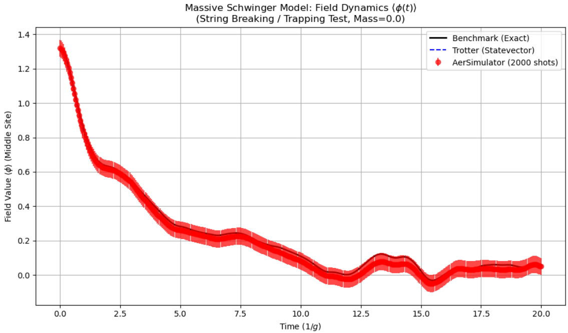

Physics: String Breaking & Screening

- **Behavior:** The field value $\langle \phi \rangle$ starts high (≈ 1.3) and decays rapidly towards zero.
- **Interpretation:** In the massless limit ($m = 0$), the vacuum can easily create fermion pairs to screen the external field. The "string" of energy breaks and dissipates into the vacuum.

Results VIII: Massive Dynamics ($m = 0.5$)

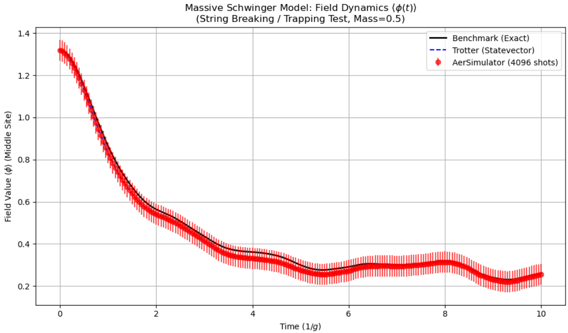

Physics: Confinement & Trapping

- **Behavior:** The field decays initially but settles into a **non-zero** oscillation ($\langle\phi\rangle \approx 0.3$). It does not vanish.
- **Interpretation:** The mass term acts as a confining potential. Pair production is energetically costly ($2m$), so the field is "trapped" or confined, unable to fully dissipate.

Discussion: Screening vs. Confinement

1. **Massless Case (Screening)**
   - Corresponds to a free massive scalar boson (mass $\mu = e/\sqrt{\pi}$).
   - The electric flux tube is unstable and is completely screened by the vacuum polarization.
2. **Massive Case (Confinement)**
   - Governed by the Sine-Gordon potential $\sim \cos(2\sqrt{\pi}\phi)$.
   - Fractional charges or strong fields cannot be fully screened.
   - The persistent oscillation signifies a stable "string" or confined state that cannot decay into free particles.

Method Validation

The plots demonstrate the accuracy of the quantum simulation methods against the exact solution.

- **Benchmark (Black Line):** Exact matrix exponentiation.
- **Trotter (Blue Dashed):** The quantum circuit approximation ($dt = 0.05$) introduces negligible error, tracking the exact dynamics perfectly.
- **Aer Simulator (Red Dots):** Even with shot noise (2000-4096 shots), the quantum measurements accurately capture the subtle differences between decay (massless) and trapping (massive).

Results IX: Meson Scattering

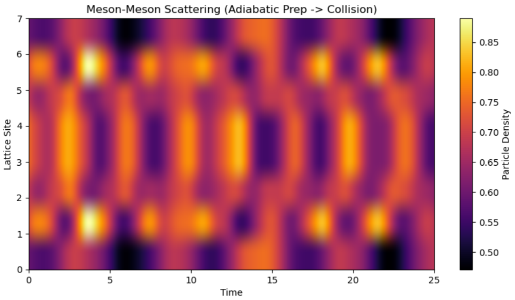

Simulating Particle Collisions on a Lattice

- **Protocol:** Two meson wavepackets are initialized with opposite momenta $(k, -k)$ and adiabatically "dressed" to turn on interactions. [4, 5]
- **Observation:** The heatmap shows the density profiles converging, creating a high-density interaction region at the center, and subsequently scattering.

Results X: Dynamic Screening & Particle Production

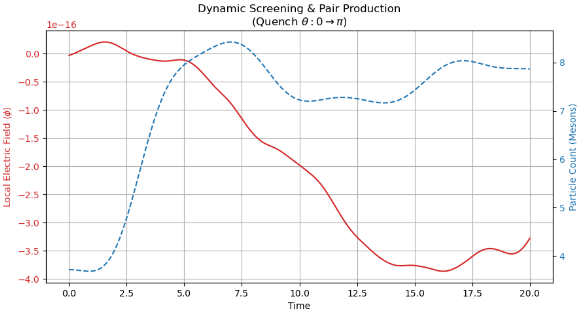

Quench Dynamics ($\theta : 0 \to \pi$)

- **Field Decay (Red):** The local electric field $\langle \phi \rangle$ oscillates and decays as the vacuum polarizes to screen the background field.
- **Pair Production (Blue):** The total particle count rises significantly, confirming that field energy is being converted into matter (Meson pairs).

Results XI: Perturbation Theory Limits

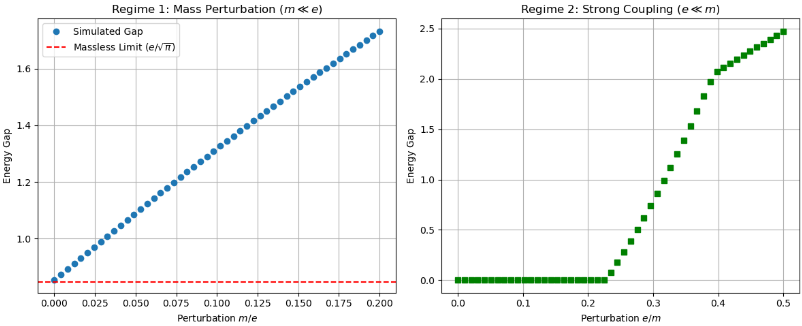

Validation against Analytical Limits

- **Left ($m \ll e$):** The energy gap converges to the analytic massless Schwinger boson mass $M = e/\sqrt{\pi}$ (Red Line) as the fermion mass $m \to 0$.
- **Right ($e \ll m$):** In the strong coupling/massive limit, the gap scales linearly, approaching the free massive fermion limit ($2m$).

Results XII: Static Potential & Confinement

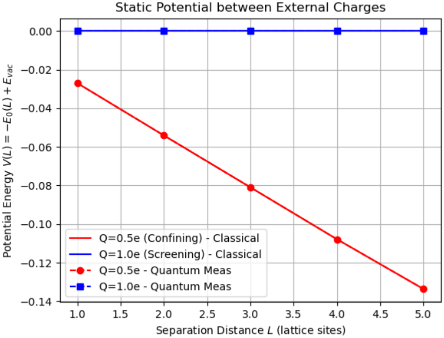

Screening vs. Confinement

- **Integer Charge ($Q = 1.0$, Blue):** The potential is flat, showing that the vacuum screens integer charges.
- **Fractional Charge ($Q = 0.5$, Red):** The potential drops linearly ($V \propto L$), indicating a confinement.
- **Validation:** Quantum measurements (markers) match classical theory (lines) perfectly.

Results XIII: Entanglement Entropy Dynamics

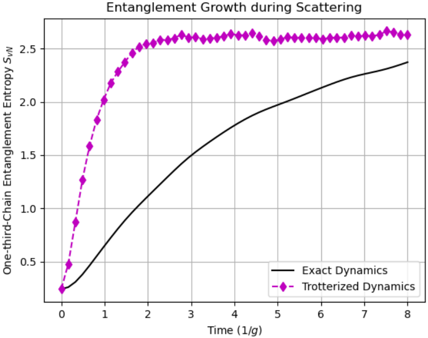

Entanglement Growth during Collision

- **Growth:** Entropy S_{vN} rises sharply during the collision $(t \approx 1 - 4)$, quantifying the generation of quantum entanglement.
- **Saturation:** Post-collision, entropy stabilizes at a non-zero value (≈ 2.5), indicating permanent entanglement between scattered products.

Results XIV: High-Energy Scattering Limits

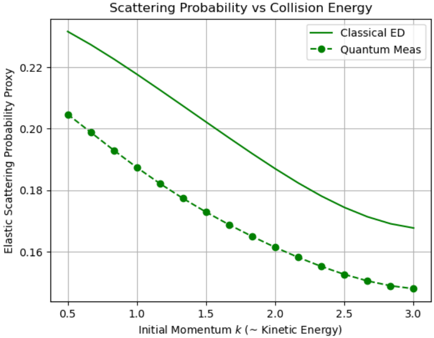

Elastic Scattering vs. Kinetic Energy

- **Trend:** Elastic scattering probability decreases as momentum k increases, consistent with inelastic particle production at high energies.
- **Simulation Limits:** The deviation of Quantum results from Classical at high k highlights Trotter error accumulation.

Thank you

Questions?

Extra Results I: Vacuum Structure & Phase Transitions

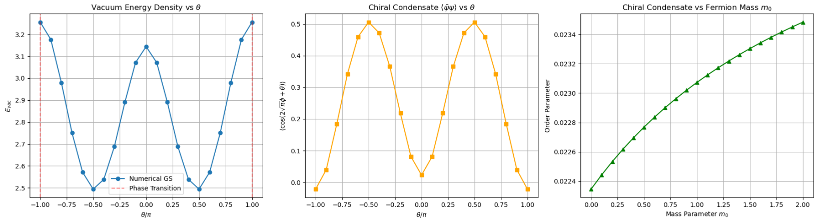

Left: Vacuum Energy Density vs θ.

Center: Chiral Condensate Σ vs θ.

Right: Chiral Condensate vs Mass m_0.

Discussion: The θ-Vacuum & Phase Transition

1. **Periodicity Topology**
   - The vacuum energy $E_{vac}(\theta)$ is periodic in 2π, reflecting the topological structure of the $U(1)$ gauge group.
   - Integer external charges ($\theta = 0, 2\pi$) are fully screened by the vacuum.

2. **Phase Transition at $\theta = \pi$**
   - Energy Cusp: At $\theta = \pi$, the ground state energy exhibits a sharp cusp (non-differentiable point).
   - Order Parameter Discontinuity: The Chiral Condensate $\langle \bar{\psi}\psi \rangle$ jumps discontinuously at $\theta = \pi$.
   - Physical Interpretation: This indicates a *first-order phase transition* associated with the spontaneous breaking of CP symmetry.

Methodology I: Lattice Discretization (Setup)

The continuous field is mapped to a lattice of truncated harmonic oscillators (bosonic basis).

1. System Parameters (`params`)

- Lattice Size: $N = 9$ sites (Open Boundary).
- Hilbert Space Truncation: $N_{levels} = 4$ per site.
- Qubit Mapping: $\lceil \log_2(4) \rceil = 2$ qubits per site $\rightarrow$ 18 total qubits.

2. Operator Mappings (`SchwingerOperators`) The scalar field ϕ and momentum π are constructed from creation/annihilation operators $(a, a^\dagger)$ truncated at level 3:

$$\phi_j = \frac{1}{\sqrt{2W_0}}(a_j + a_j^\dagger) \tag{11}$$

$$\pi_j = -i\sqrt{\frac{W_0}{2}}(a_j - a_j^\dagger) \tag{12}$$

where $W_0 = 1.0$ is the reference frequency.

Methodology II: Hamiltonian Engineering

The Hamiltonian is constructed via sparse matrices (Benchmark) and Pauli strings (Quantum).

1. Total Hamiltonian Components The code implements the bosonized Hamiltonian summing three terms:

- **Kinetic (H_K):** $\sum_j \frac{A}{2}\pi_j^2$
- **Mass + Gradient (H_M):** $\sum_j \left(\frac{A\mu^2}{2} + \frac{1}{A}\right)\phi_j^2$
- **Interaction (H_{int}):** $-\sum_j \frac{1}{A}(\phi_j\phi_{j+1})$

Note: The gradient term $(\phi_{j+1} - \phi_j)^2$ is expanded into local ϕ^2 and nearest-neighbor $\phi_j\phi_{j+1}$ terms.

2. Trotter Decomposition First-order Trotter-Suzuki expansion with $dt = 0.05$:

$$U(dt) \approx e^{-iH_{int}dt}e^{-iH_M dt}e^{-iH_K dt} \tag{13}$$

Implemented using Qiskit's `PauliEvolutionGate`.

Methodology III: State Preparation & Execution

1. **State Preparation (`get_initial_state_vector`)** Initial states are created using the Displacement Operator $D(\alpha) = e^{\alpha a^\dagger - \alpha^* a}$ on the vacuum $|0\rangle$, with magnitude $\alpha = 1.5$.
   - **System 1 (String):** $D(\alpha)$ applied to sites $j \in [3, 5]$.
   - **System 2 (Step):** $D(\alpha)$ applied to sites $j \geq 4$.
2. **Execution Protocol**
   - **Benchmark:** Exact sparse matrix exponentiation (`expm_multiply`).
   - **Trotter (Statevector):** Noiseless statevector evolution.
   - **Quantum (Shots):** `EstimatorV2` primitive with 2000 shots. Measures local field expectation values $\langle \phi_j \rangle$ at every time step.

Results that confuse me I

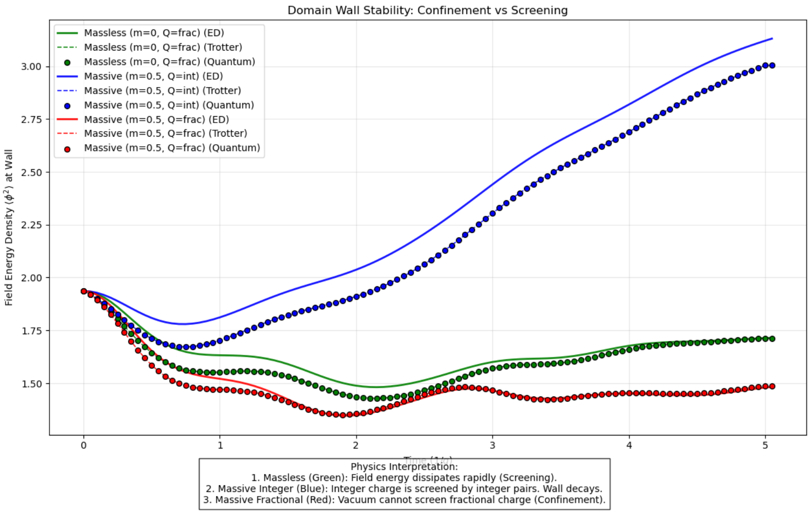

Energy squared of domain wall with time

Results that confuse me II

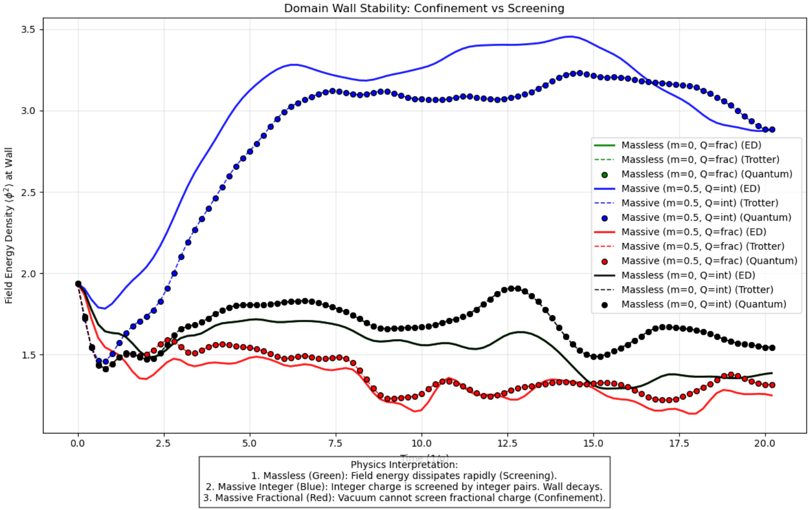

Energy squared of domain wall with time

References I

[1] Satoshi Iso and Hitoshi Murayama. "ALL ABOUT THE MASSLESS SCHWINGER MODEL". In: (July 1988).

[2] Sidney Coleman, R Jackiw, and Leonard Susskind. "Charge shielding and quark confinement in the massive schwinger model". In: *Annals of Physics* 93.1 (1975), pp. 267–275. ISSN: 0003-4916. DOI: https://doi.org/10.1016/0003-4916(75)90212-2. URL: https://www.sciencedirect.com/science/article/pii/0003491675902122.

[3] Sidney Coleman. "More about the massive Schwinger model". In: *Annals of Physics* 101.1 (1976), pp. 239–267. ISSN: 0003-4916. DOI: https://doi.org/10.1016/0003-4916(76)90280-3. URL: https://www.sciencedirect.com/science/article/pii/0003491676902803.

References II

[4] Ron Belyansky et al. "High-Energy Collision of Quarks and Mesons in the Schwinger Model: From Tensor Networks to Circuit QED". In: *Phys. Rev. Lett.* 132 (9 Feb. 2024), p. 091903. DOI: 10.1103/PhysRevLett.132.091903. URL: https://link.aps.org/doi/10.1103/PhysRevLett.132.091903.

[5] Zohreh Davoudi. "TASI/CERN/KITP Lecture Notes on "Toward Quantum Computing Gauge Theories of Nature"". In: (July 2025). arXiv: 2507.15840 [hep-lat].